PCCP

PAPER

View Article Online
View Journal | View Issue

Cite this: *Phys. Chem. Chem. Phys.*, 2018, **20**, 9838

Mechanism of ionic-liquid-based acidic aqueous biphasic system formation†

Nicolas Schaeffer,[a] Helena Passos,[a] Matthieu Gras,[b] Vijetha Mogilireddy,[b] João P. Leal,[c] Germán Pérez-Sánchez,[a] José R. B. Gomes,[a] Isabelle Billard,[b] Nicolas Papaiconomou[b] and João A. P. Coutinho*[a]

Received 8th February 2018,
Accepted 8th March 2018

DOI: 10.1039/c8cp00937f

rsc.li/pccp

Ionic-liquid-based acidic aqueous biphasic systems (IL-based AcABS) represent a promising alternative to the solvent extraction process for the recovery of critical metals, in which the substitution of the inorganic salt by an acid allows for a 'one-pot' approach to the leaching and separation of metals. However, a more fundamental understanding of AcABS formation remains wanting. In this work, the formation mechanisms of AcABS are elucidated through a comparison with traditional aqueous biphasic systems (ABS). A large screening of AcABS formation with a wide range of IL identifies the charge shielding of the cation as the primary structural driver for the applicability of an IL in AcABS. Through a systematic study of tributyltetradecylphosphonium chloride ($[P_{44414}]Cl$) with various chloride salts and acids, we observed the first significant deviation to the cationic Hofmeister series reported for IL-based ABS. Furthermore, the weaker than expected salting-out ability of H_3O^+ compared to Na^+ is attributed to the greater interaction of H_3O^+ with the $[P_{44414}]^+$ micelle surface. Finally, the remarkable thermomorphic properties of $[P_{44414}]Cl$ based systems are investigated with a significant increase in the biphasic region induced by the increase in the temperature from 298 K to 323 K. These finding allows for the extension of ABS to new acidic systems and highlights their versatility and tunability.

Introduction

In recent years, ionic liquids (ILs) have attracted significant interest in the field of metal extraction as an alternative medium in solvent extraction processes. ILs are salts composed of asymmetric ions with disperse charge that are liquid at room temperature. Since the proposal of ILs as environmentally friendly media to replace volatile organic solvents for liquid–liquid extraction,[1] the use of ILs for solvent extraction has been a widely studied field in IL mediated metal processing. Solvent extraction is the favoured option for metal separation and involves the preferential distribution of a solute between two mutually immiscible liquid phases, usually consisting of an aqueous acidic solution and an aliphatic organic solvent. ILs used in solvent extraction operations must be water immiscible to promote the recovery of the metal and minimize the loss of the IL to the aqueous phase.

The interest for the application of ILs in solvent extraction processes stems from their ionic nature, which results in metal extraction mechanisms not possible in conventional organic solvents. The ability of ILs to solvate both charged and neutral metal complexes is the reason behind the various reported extraction mechanisms in IL mediated solvent extraction processes.[2] The capacity of ILs to extract charged metal complexes can result in different extraction mechanisms compared to traditional solvent extraction processes in which only neutral metal–ligand complexes can transfer from the aqueous to the hydrophobic phase. Furthermore, through careful manipulation of the cation and anion selection and design, the properties of ILs can be tailored to exhibit a high selectivity for a specific metal.[3,4]

Despite these promising aspects, several factors limit the industrial application of ILs in solvent extraction processes. The available range of hydrophobic ILs is limited by the structural modifications that confer their hydrophobicity, namely the incorporation of fluorinated moieties or long alkyl chains in the cation or anion. ILs based on fluorinated anions such as bis(trifluoromethanesulfonyl)imide, $[NTf_2]^-$, are expensive, toxic[5] and exhibit increased solubility in inorganic acids.[6,7] ILs composed of long hydrophobic alkyl chains exhibit high viscosities, particularly after metal extraction, that hinder their industrial applicability.[8]

We recently demonstrated that many of these issues could be overcome through the application of acidic aqueous biphasic

[a] *CICECO, Department of Chemistry, University of Aveiro, Campus Universitário de Santiago, 3810-193 Aveiro, Portugal. E-mail: jcoutinho@ua.pt*
[b] *LEPMI – Universite Grenoble-Alpes, F-38000 Grenoble, France*
[c] *C2TN, DECN, Instituto Superior Técnico, Universidade de Lisboa, 2695-066 Bobadela, Portugal*

† Electronic supplementary information (ESI) available. See DOI: 10.1039/c8cp00937f

systems (AcABS) for metal extraction.[9] Aqueous biphasic systems (ABS) represent a well-established alternative to solvent extraction for the separation and purification of target compounds. They are primarily composed of water and a water-soluble low-polarity solute, which upon addition, in the right proportions, of an inorganic salt partition to form a reversible biphasic system composed of a salt-rich phase and an organic-rich phase. In the newly reported AcABS composed of tributyltetradecylphosphonium chloride ($[P_{44414}]Cl$), HCl and H_2O, the inorganic salt is replaced by the acid used to leach the metals.

To increase the applicability of AcABS to a wider range of ILs and metal extraction matrices, an understanding of the phase behaviour of ILs in aqueous solutions with inorganic acids on a molecular level is required. However, the use of acidic solutions in conjunction with IL-based ABS is traditionally avoided due to the increased solubility of ILs in inorganic acids[6,7] and the consequential reduction of the biphasic region with decreasing pH.[10] As such, a detailed understanding of the interactions between water soluble ILs and inorganic acid is still lacking. In this work, we attempt to understand the molecular mechanisms driving AcABS formation and compare them to those controlling the formation of traditional ABS. Furthermore, the flexibility of AcABS is demonstrated through its temperature behaviour, and structural guidelines are given for the suitability of various commercial ILs to form AcABS.

Methodology

Materials and instrumentation

The ABS studied in this work were established by various aqueous solutions of HCl (37 wt% from Sigma-Aldrich), LiCl (99 wt% pure from Merck), NaCl (99.9 wt% pure from BDH Chemicals), KCl (99.5 wt% pure from Chem-Lab), CsCl (99.5 wt% pure from Panreac), $MgCl_2$ (99 wt% pure from Merck) and $CaCl_2$ (99 wt% pure from Panreac), and different aqueous solutions of hydrophilic ILs. A total of 48 commercially available hydrophilic ILs were evaluated for AcABS formation with variation in the cation and anion structures. These include 1-alkyl-3-methylimidazolium ($[C_n mim]^+$ (n = 2–14)), 1-butylmethylpiperidinium ($[C_4mpip]^+$), 1-butylpyridinium ($[C_4py]^+$), 1-butylpyrrolidinium ($[C_4pyrr]^+$), tetraalkylammonium ($[N_{R1R2R3R4}]^+$), tetraalkylphosphonium ($[P_{R1R2R3R4}]^+$) and cholinium ($[Ch]^+$) based ILs with various anions including chloride, bromide, nitrate, alkyl sulfate ($[C_nSO_4]^-$ (n = 0–2)), dihydrogen phosphate ($[H_2PO_4]^-$), ethyl phosphate ($[C_2H_5PO_4]^-$), di-ethyl phosphate ($[(Et)_2PO_4]^-$), tetrafluoroborate ($[BF_4]^-$), thiocyanate ($[SCN]^-$), dicyanamide ($[N(CN)_2]^-$), tosylate ($[Tos]^-$), acetate ($[CH_3CO_2]^-$), trifluoroacetate ($[CF_3CO_2]^-$), mesylate ($[CH_3SO_3]^-$) and triflate ($[CF_3SO_3]^-$) anions. A summary of the chemical structures for the ILs investigated is presented in Fig. 1 and the full list is provided in Table S1 of the ESI.† All ILs were purchased from Iolitec and were used as received. $[P_{44414}]Cl$ and $[P_{4444}]Br$ were of 95 wt% purity; all other ILs were 97–99 wt% pure. Nitric acid (65 wt%), sulfuric acid (95 wt%) and phosphoric acid (85 wt%) were acquired from Chem-Lab, Sigma-Aldrich and Panreac, respectively. NaOH (98 wt%) was purchased from Eka.

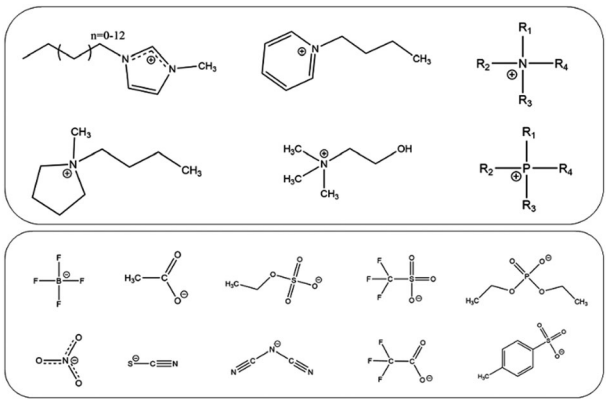

Fig. 1 Chemical structures of the main cations and anions considered for AcABS formation. The full list is presented in Table S1 of the ESI.†

Ultrapure, double distilled water, passed through a reverse osmosis system and further treated with a Milli-Q plus 185 water purification apparatus, was used for all experiments. Hexahydrate cobalt and nickel chloride salts were purchased from Merck (99 wt% pure).

Electrospray ionization mass spectrometry (ESI-MS) analysis was performed using a Bruker HCT quadrupole ion trap mass spectrometer. Sample solutions were introduced to the ESI source at a flow rate of 300 μL min^{-1}, the heated capillary temperature was set to 523 K and the cover gas (N_2) to a flow rate of 2 L min^{-1}. Both positive and negative modes were detected to see the existing cations and anions. The $[P_{44414}]^+$ concentration was analysed using ^{1}H-NMR with benzene as internal standard (300 MHz Bruker Avance III spectrometer). Solution pH and conductivity were monitored using a Seven-Excellence multiparameter pH/conductivity meter (Mettler Toledo). The micelle diameter and zeta potential were obtained using a Malvern Zetasizer Nano ZS.

AcABS screening, phase diagrams and surfactant characterisation

Each IL was tested for its potential in AcABS using four inorganic acids: HCl, HNO_3, H_2SO_4 and H_3PO_4. For each IL tested, an initial mixture composed of 1 : 1 wt ratio of IL : H_2O (1 g) was prepared to which the undiluted acid was added dropwise in an ice bath to control the exothermic addition of acids. After each addition, the samples were slowly warmed in a thermostatic bath at 298 K under agitation and the process was repeated until a two-phase system appeared. AcABS was deemed to not form once the IL concentration in the system decreased below 5 wt% or visible degradation of the IL occurred. Each experiment was performed in duplicate. It must be emphasised that HNO_3 and H_2SO_4 are strong oxidants and that the stability of an IL in contact with such acids greatly depends on the ease of oxidation of their anion. In particular, ILs containing bromide, thiocyanate and dicyanamide anions all exhibited signs of degradation after contacting with concentrated HNO_3 and H_2SO_4.

Aqueous solutions of $[P_{44414}]Cl$ (50 wt%), concentrated HCl (37 wt%) and saturated solutions of chloride salts were prepared

and used for the determination of the binodal curves. The ternary system compositions were determined by the weight quantification of all components added within an uncertainty of $\pm 10^{-3}$ g. The phase diagrams were determined through the cloud point titration method in a temperature-controlled cell at 298 and 323 K under agitation and atmospheric pressure. The detailed experimental procedure adopted has been described in a previous work.[11] The surfactant properties of $[P_{44414}]Cl$ were characterised by conductometry and light scattering using a Malvern Zeta Sizer. To a 10 mL solution of ultrapure water in a temperature-controlled cell, a 60 mM solution of $[P_{44414}]Cl$ in ultrapure water was added dropwise and the weight and conductivity were recorded after each addition. Light scattering measurements were performed using ultrapure water at 298 K, with each solution analysed five separate times over a 2 h period to ensure the formation of stable aggregates.

Simulation details

Density functional theory (DFT) calculations were carried out employing Gaussian 09[12] using Becke's[13] three-parameter exchange in combination with the Lee, Yang and Parr correlation functional (B3LYP).[14] All elements were computed employing a 6-311+G(d,p) basis set. Default Gaussian 09 optimisation convergence criteria of 10^{-7} on the density matrix and 10^{-5} on the energy matrix were used. The numerical integration grid was improved from the default option to a pruned (optimized) grid of 99 radial shells and 590 angular points per shell (keyword int = ultrafine). All structures were fully optimized without symmetry constraints and confirmed as minima by vibrational analysis. Electrostatic potential surfaces were generated using Gaussview.[15]

Results and discussion

AcABS formation – the role of the ionic liquid cation

To determine the structural factors driving the AcABS behaviour, 48 commercially available ILs were evaluated at 298 K in conjunction with four inorganic acids: HCl, HNO_3, H_2SO_4 and H_3PO_4. The full list as well as their ability to form AcABS is presented in Table S1 of the ESI.† A summary of the various IL cation and anion variation studied is presented in Fig. 1.

Of all the ILs studied, only those with quaternary ammonium or phosphonium cations were able to undergo liquid–liquid demixing in the presence of inorganic acids. ILs containing a heterocycle in their structure such as imidazolium-, pyrrolidinium- or piperidinium- and pyridinium-based cations did not form AcABS regardless of the cationic alkyl chain length or anion selection. For $[C_n\text{mim}]$-based ILs, the alkyl chain length was varied from $n = 2$ to $n = 14$ with no influence on the ability of the IL to undergo separation. A systematic study of the system HNO_3 with $[N_{nnnn}]Cl$ (n = 1–5, 8) indicates that AcABS formation only occurs for $n \geq 3$. In addition, $[P_{11114}]Br$ was unable to form AcABS with any of the tested acids whilst $[P_{44414}]Cl$ was identified as the most versatile IL for AcABS application, forming AcABS with HCl, H_2SO_4 and HNO_3. This indicates that for the ILs tested, their ability to form ABS with inorganic acids is primarily a cation dependent process. The inability of cyclic cations to form AcABS is further underlined by the fact that their hydrophobic counterparts containing fluorinated anions exhibit a notable increase in aqueous solubility in the presence of inorganic acids such as HNO_3 and HCl.[6,7] In contrast, the capacity of some tetraalkylphosphonium- and ammonium-based ILs to phase separate using inorganic acids as salting-out agents is unexpected. In traditional ABS, there is a decrease in the ability for ABS formation at more acidic pH values for all conventional ILs, *i.e.* the more alkaline the pH of the aqueous medium, the larger the biphasic region for a given system.[10]

The experimental results (Table S1, ESI†) suggest that the ability of an IL to form AcABS is correlated to the cation's apparent charge density at its solvent-accessible charge surface, illustrated in Fig. 2, and not only to the cation's molar volume (hydrophobicity). A comparison of the electrodensity at the molecular surfaces of $[C_4\text{mim}]^+$, $[P_{1114}]^+$ and $[P_{4444}]^+$ cations (Fig. 2) clearly shows that $[C_4\text{mim}]^+$ and $[P_{1114}]^+$ possess an easily solvent accessible charge centered around the acidic hydrogen attached to the C^2 carbon between the two nitrogen atoms in the ring in the case of $[C_4\text{mim}]^+$ and the trimethylphosphonium polar region for $[P_{1114}]^+$. In contrast, the four butyl chains surrounding the phosphonium center effectively shield the cationic charge from the solvent, resulting in a more neutral surface charge (*cf.* compare larger greener regions in the rightmost panel of Fig. 2 with the larger bluish regions in the two other panels).

This variation in charge accessibility amongst various cations is also reflected in the ability of a cation to hydrogen bond with water. The Kamlet–Taft α parameter describes the ability of a solvent to donate a proton in a solvent-to-solute hydrogen bond, with the fixed reference point of $\alpha = 1$ for methanol.[16] The hydrogen bond donor ability of an IL is primarily controlled by the cation; by keeping the anion constant any variation in α can be solely attributed to cationic effects.[17] The ability of a cation to promote phase separation is closely related with its ability to hydrogen bond with water, with lower values of α indicative of easier liquid–liquid demixing. The α parameters for a range of representative ILs (comprising no functional groups) are presented in Table 1. In decreasing order of α values, imidazolium ILs have greater α values followed by pyridinium, pyrrolidinium and ammonium ILs, with phosphonium-based ILs having the

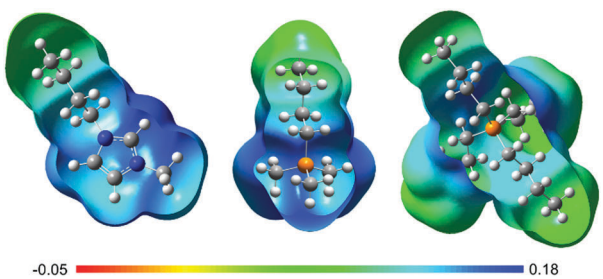

Fig. 2 Comparison of the charge distribution at the molecular surface of $[C_4\text{mim}]^+$, $[P_{1114}]^+$ and $[P_{4444}]^+$ cations computed at the B3LYP/6-311+G(d,p) level of theory. Blue color illustrates positively charge segments while red color illustrates negatively charged segments.

Table 1 Predicted Kamlet–Taft parameter α for selected $[NTf_2]$-based ILs based on linear regression of COSMO-RS simulation parameters[18]

Ionic liquid	Cation	α
$[C_4mim][NTf_2]$	1-Methyl-3-butylimidazolium	0.692
$[C_4py][NTf_2]$	1-Butylpyridinium	0.680
$[C_4mpyrr][NTf_2]$	1-Methyl-1-butylpyrrolidinium	0.433
$[N_{1111}][NTf_2]$	Tetramethylammonium	0.759
$[N_{2222}][NTf_2]$	Tetraethylammonium	0.403
$[N_{3333}][NTf_2]$	Tetrapropylammonium	0.327
$[N_{4444}][NTf_2]$	Tetrabutylammonium	0.291
$[N_{4111}][NTf_2]$	Butyltrimethylammonium	0.583
$[P_{4444}][NTf_2]$	Tetrabutylphosphonium	0.292

lowest of all. When considering the trend in α values from $[N_{1111}]^+$ to $[N_{4444}]^+$, a shift is observed moving from $[N_{2222}]^+$ to $[N_{3333}]^+$. This corresponds to the experimental limit of AcABS formation for the $[N_{nnnn}]Cl$ (n = 1–5, 8) and HNO_3 systems.

From the results presented in Table S1 (ESI†), Table 1 and Fig. 2, charge shielding of the cation appears as the primary factor determining the eligibility of an IL for AcABS, with results indicating propyl as the minimal alkyl chain length for tetra-alkylammonium- and phosphonium-based ILs to undergo liquid–liquid demixing in the presence of acids. Recent results by Silva *et al.*[19] appear to further validate this conclusion. Their work shows that $[N_{1111}]Cl$ and $[N_{2222}]Cl$ behaved like Coulombic-dominated salts whilst the behaviour of $[N_{nnnn}]Cl$ for n = 3–4 was closer to that of a traditional IL, based on the trend in the phase-forming abilities of these ILs to create ABS with poly(ethylene)glycol. Having demonstrated the determinant factor for AcABS formation, the remaining of this report will focus on $[P_{44414}]Cl$ which was identified as capable of forming an AcABS with HCl, H_2SO_4 and HNO_3.

AcABS formation – the role of the acid

To fully understand the factors driving AcABS formation, the behaviour of concentrated acids in IL solutions must be addressed, namely their speciation and the probability of anion exchange with the IL anion. Of the four acids tested, HNO_3 was identified as the strongest phase former followed by H_2SO_4, HCl and finally H_3PO_4, which was unable to induce AcABS with any of the tested ILs. This inability of H_3PO_4 to form AcABS and the ability of nitric acid to induce AcABS formation is unexpected, since for traditional ABS the ability to induce phase separation for a salt series with common cation follows the order $PO_4^{3-} > SO_4^{2-} > Cl^- \gg NO_3^-$ in accordance with the Hofmeister series.[20] However, previous research has shown that the phase behaviour of IL-based ABS with polyvalent salts is heavily dependent on their speciation in aqueous solutions.[21] A similar consideration must thus be taken into account when discussing the role of acids with multiple protons. HCl and HNO_3 both have acid dissociation constants (pK_a) values below −1 and can thus be considered as fully dissociated even in concentrated acid solutions to H_3O^+ and Cl^- or H_3O^+ and NO_3^-, respectively.[22] In contrast, H_2SO_4 can dissociate in two species, HSO_4^- ($pK_a < -1$) and SO_4^{2-} ($pK_a \approx 2$), whilst H_3PO_4 can exist as either $H_2PO_4^-$ ($pK_a \approx 2$), HPO_4^{2-} ($pK_a \approx 7$) or HPO_4^{2-} ($pK_a \approx 12$) depending on the pH.[22] The pH of AcABS in all cases is below 0.5. Under these conditions, the prevalent species in H_2SO_4- and H_3PO_4-based AcABS are therefore HSO_4^- and $H_3PO_4/H_2PO_4^-$ respectively. The inability of phosphoric acid to fully dissociate under the acidic conditions required for AcABS explains its ineffectiveness compared to the other acids tested.

Table 2 Main positive and negative peaks of the $[P_{44414}]^+$-based rich phase at the binodal concentration for the $[P_{44414}]Cl–H_2O–X$ (X = HCl, H_2SO_4, and HNO_3) systems

Total solution composition	m/z (relative intensity)	Band assignment
18.6 wt% IL	Positive	
19.6 wt% HCl	399 (100%)	$[P_{44414}]^+$
61.8 wt% H_2O	Negative	
	469 (100%)	$[(P_{44414})(Cl)_2]^-$
33.2 wt% IL	Positive	
15.8 wt% H_2SO_4	399 (100%)	$[P_{44414}]^+$
51.0 wt% H_2O	Negative	
	593 (33%)	$[(P_{44414})Cl(HSO_4)]^-$
	789 (16.5%)	$[(P_{44414})(HSO_4)_2(H_2SO_4)]^-$
37.8 wt% IL	Positive	
2.9 wt% HNO_3	834 (100%)	$[(P_{44414})_2Cl]^+$
59.3 wt% H_2O	861 (21.1%)	$[(P_{44414})_2(NO_3)]^+$
	Negative	
	523 (100%)	$[(P_{44414})(NO_3)_2]^-$

Having established that the three acids able to induce AcABS all dissociate into the monovalent anions HSO_4^-, Cl^- and NO_3^-, the extent of anion-exchange was investigated. Starting from 40 wt% $[P_{44414}]Cl$ solutions in H_2O, undiluted HCl, H_2SO_4 and HNO_3 were added respectively until the formation of a biphasic system occurred. The phases were left to separate prior to analysis of the IL-rich phase (upper phase) by ESI-MS, with the results presented in Table 2.

The results indicate that partial ion exchange occurs between Cl^- and HSO_4^-, while close to quantitative ion exchange was observed with Cl^- and NO_3^- respectively. This metathesis reaction is in accordance with the Hofmeister series in which anions with a lower charge density such as NO_3^- are less well hydrated, therefore more hydrophobic, which leads to a greater affinity for the IL-rich phase. In contrast, more hydrophilic anions such as Cl^- prefer the aqueous phase in which they are better solvated.[23] The increased hydrophobic character of NO_3^- *versus* Cl^- is further validated by the fact that the resulting $[P_{44414}][NO_3]$ IL is no longer fully miscible in water. As such, care must be taken when discussing AcABS with nitric acid as the salting-out agent due to the occurrence of ion-exchange which appears to be the primary driver of biphasic system formation. The HSO_4^- exhibits a behaviour intermediate between those of the other two anions and as such only partial substitution with the chloride anion is observed.[20,23] In the following discussions, only chloride-based salts and $[P_{44414}]Cl$ are used in order to eliminate the additional complexity of anion-exchange when examining AcABS formation mechanisms.

Comparison of ABS *versus* AcABS – establishment of a cationic series

In order to further investigate AcABS formation and compare the latter to traditional ABS, the experimental phase diagrams

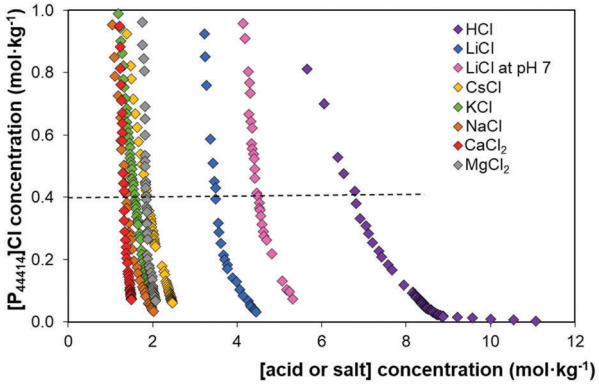

Fig. 3 Binodal curves for the ABS and AcABS composed of HCl, LiCl, NaCl, KCl, CsCl, $MgCl_2$ and $CaCl_2$ with $[P_{44414}]Cl$ at 298 K.

for $[P_{44414}]Cl$ with HCl, LiCl, NaCl, KCl, CsCl, $CaCl_2$ and $MgCl_2$ were determined at 298 K (Fig. 3). To enable a comparison between the different salts, all concentrations are reported in molality units (mol kg^{-1} of solvent).

The shapes of the experimental binodal curves in Fig. 3 are interesting for two reasons. Firstly, with the exception of HCl and to a lesser extent LiCl, all binodal curves are approximately linear, almost vertical, for a large range of $[P_{44414}]Cl$ concentrations. This indicates that above a certain salt concentration, the system behaves more like the binary hydrophobic–hydrophilic phases in solvent extraction processes than as a conventional ABS in which the concentration of salt to induce phase demixing varies with the IL concentration.[11] Secondly, all binodal curves run down to the horizontal axis, suggesting that negligible $[P_{44414}]Cl$ concentrations are present in the acid/salt-rich phase. This is important from a recycling perspective, ensuring that minimal IL is lost between each recovery stage.

To compare the efficacy of the various salts to induce phase separation, the arbitrary $[P_{44414}]Cl$ concentration of 0.4 mol kg^{-1} (15 wt%) was selected (dotted line, Fig. 3). At this IL concentration, the ability of the tested salt to induce phase separation at 293 K follows the trend $CaCl_2$ > NaCl > KCl > $MgCl_2$ > CsCl ≫ LiCl ≫ HCl. This experimentally observed trend markedly deviates from the traditionally accepted cationic Hofmeister series for IL-based ABS, in which the molar entropy of hydration of strong water coordinating ions such as Mg^{2+} and Li^+ is the primary driving force for the aqueous two-phase system formation. High charge density ions tend to form water–ion hydration complexes that cause the dehydration of the solute and the increase of the surface tension of the ion cavity.[20] As such, divalent ions usually present a stronger salting-out ability than the monovalent ones. Whilst the sequence $CaCl_2$ > NaCl > KCl > CsCl is in accordance with the expected Hofmeister ordering, the lower salting-out ability of $MgCl_2$, LiCl and HCl for $[P_{44414}]Cl$ is not.[23] To the best of our knowledge, this represents the first significant deviation to the cationic Hofmeister series reported for the IL-based ABS. This suggests that the mechanism of AcABS formation in some cases deviates significantly from the accepted salting-out behaviour and as such, the Hofmeister series reference should be used with care as it may induce wrong predictions on experimentally unknown systems of this type.

It is important to emphasize that the Hofmeister series pertains to ions near a surface, making direct ion–macromolecule interactions more important for ion specific phenomena than bulk solution ion properties. A change in factors such as the surface charge, surface polarity, temperature, salt concentration and pH has led to the discovery of a diverse spectrum of variable series in non-IL-based ABS (proteins, colloids, surfactants, *etc.*).[24–28] For intermediate situations of hydrophobic/hydrophilic interfaces, anions and cations can change their order on the Hofmeister series sequence. Furthermore, the nature of ion–macromolecule interaction displays molecular-scale heterogeneity in line with the well-documented nano-scale ordering of IL solutions. For example, ^{1}H-NMR analysis of $[C_4mim][NTf_2]$ with various inorganic salts in aqueous solutions revealed the existence of preferential specific interactions between the low electrical charge density parts of the cation (the cationic alkyl chain) and the inorganic salts and their variation as one moves from salting-out to salting-in effects.[29] It is in this context that the special case of the $MgCl_2$/LiCl–$[P_{44414}]Cl$ systems is discussed. The AcABS HCl–$[P_{44414}]Cl$ is analysed in the next section.

The C_{14} alkyl chain confers the $[P_{44414}]^+$ cation surfactant properties in which the water accessible surface area can vary significantly, whilst the bulky $[P_{44414}]^+$ polar head 'pushes' the positive charge deeper into the cation bulk as shown in Fig. 2. This shielding of the cationic charge by the long alkyl chains results in a smaller surface charge and a more apolar cation–solvent surface, which is exacerbated by the self-organisation of the cations in aqueous solutions. X-ray photoelectron spectroscopy of the structurally similar $[P_{66614}]^+$ based IL with various anions in aqueous solution showed that the long alkyl chains are wrapped around the cationic centre effectively shielding it from 'seeing' the anion, thereby giving the cation a non-ionic character.[30] Molecular dynamics simulations of neat $[P_{44414}][NTf_2]$ found no hydrogen bond interactions for 20% of the cations, further confirming the low-interactive nature of $[P_{44414}]^+$.[31] Based on the important structural differences between $[P_{44414}]^+$ and conventional planar IL cations typically reported in ABS, it is therefore not surprising that a divergence from the traditional Hofmeister series is observed for $[P_{44414}]Cl$. Instead, the obtained trend $Na^+ \geq K^+ > Li^+$ (Fig. 3) is characteristic of the salting-out behaviour for aliphatic[32,33] and aromatic solutes.[34]

In addition, the charge-dense lithium ion often exhibits anomalous behaviour from the predicted Hofmeister series and can weaken the hydrophobic effect,[26,35] including for a non-ionic surfactant where the lithium cation was shown to interact with the polar head groups of the molecule.[36–38] Previous researchers have postulated that due to its small radius and high charge density, Li^+ possesses an inflexible first hydration shell of four water molecules which stays intact at hydrophobic interfaces in contrast to the other halide salts.[24,26] At the hydrophobic surface, the behaviour of Li^+ is of an ion with an effectively larger radius, allowing for a greater degree of interaction and a reduction in solute hydrophobicity.[26,35,39] To evaluate the applicability of the previous explanation to the studied IL, the pH of the

LiCl–[P_{44414}]Cl system presented in Fig. 3 was adjusted from its original pH of 4.5 to 7 using a 0.1 M NaOH solution. As can be observed from Fig. 3, the increase of the pH to 7 drastically decreases the size of the biphasic region, with an additional 1 mol kg^{-1} of LiCl required to induce phase separation. The pH was also adjusted to 7 for the other chloride salts with no observed changes in the position of the binodal (example for $MgCl_2$ is presented in Fig. S1 of the ESI†). In all cases the addition of NaOH in the solution represents less than 0.5 wt% of the system. This singular decrease in the binodal region confirms the anomalous behaviour of Li^+ compared to the other tested salts in conjunction with [P_{44414}]Cl.

A similar explanation to that of Li^+ is postulated for the lower than expected hydrophilic effect of Mg^{2+} with [P_{44414}]Cl. Mg^{2+} is a small cation with an ionic radius of ~0.65 Å, only marginally larger than that of Li^+ (~0.60 Å).[40] The strong electrostatic interactions between Mg^{2+} and the surrounding water dipoles results in a highly ordered first hydration shell consisting of six water molecules arranged in a well-described octahedral geometry.[41] This tight first hydration shell in some cases allows Mg^{2+} to reside closer to hydrophobic interfaces compared to Ca^{2+}. For example, the greater ability of Mg^{2+} to polarize surrounding water molecules compared to Ca^{2+} is the key determinant in the selectivity of cellular Mg^{2+} ion channels and transporters which rely on the stronger Mg^{2+}–water–protein interactions.[42] However, no variation in the position of the binodal was encountered after pH adjustment to 7 in contrast to Li^+, suggesting the contribution of other unaccounted factors. This includes the important effect of temperature discussed further on.

Comparison of ABS *versus* AcABS – the role of H_3O^+

In this section, the behaviour of the AcABS HCl–[P_{44414}]Cl is analysed and compared to that of NaCl–[P_{44414}]Cl. The conductivity measurement of [P_{44414}]Cl at 298 K indicates that the behaviour of the [P_{44414}]$^+$ cation in aqueous solution is typical of that of a surfactant with the formation of spherical micelles above its critical micelle concentration (cmc) of 3.3 mM (Fig. 4A). The low charge density of the polar head [P_{44414}]$^+$ minimises the electrostatic repulsion between neighbouring headgroups allowing for van der Waals dispersion forces to dominate the aggregation behaviour. However, [P_{44414}]Cl does retain some qualities of cationic surfactants with zeta-potential measurements indicating an apparent micelle charge of 8.8 mV (±2.3 mV) for a [P_{44414}]Cl solution concentration near the cmc (8.1 mM).

It is well known that micelle properties are affected by the nature of monatomic ions, with these effects becoming more evident as the ion adsorption at the interface increases.[43] For a fixed [P_{44414}]Cl concentration of 20 wt% at 298 K, the addition of dilute amounts of NaCl and HCl respectively has different effects on the self-organisation of the IL cation (Fig. 4B). The presence of NaCl causes (i) an increase in the size of the micelles from 9 nm at 2 wt% to approximately 55 nm at 7 wt% and (ii) the compaction of the micelle (narrower micelle diameter distribution). In contrast, the addition of HCl has a much lower impact on micelle growth with no significant change in the micelle diameter as the concentration is increased

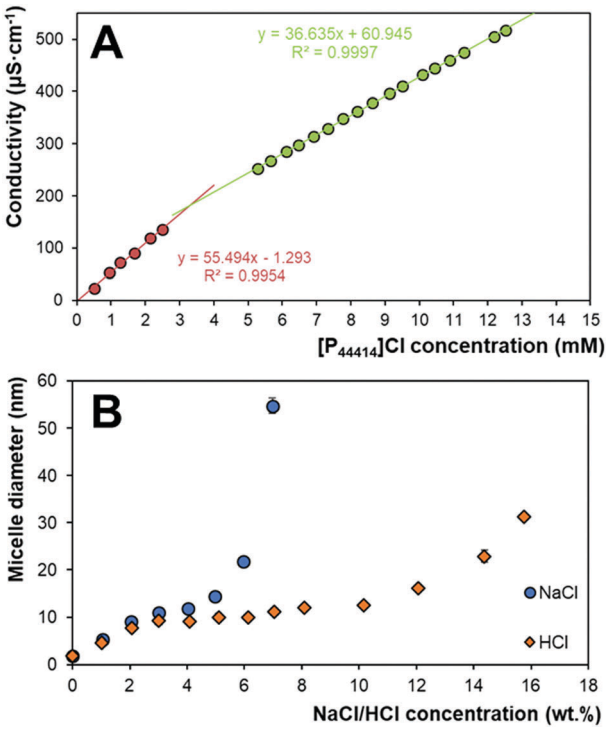

Fig. 4 (A) Variation in the conductivity of aqueous [P_{44414}]Cl solutions at 298 K as a function of [P_{44414}]Cl concentration. (B) Influence of NaCl and HCl concentrations on the [P_{44414}]$^+$ micelle diameter in 20 wt% [P_{44414}]Cl solution at 298 K.

from 2 wt% to 12 wt%. In this concentration range, HCl appears to drive the growth in the number of spherical aggregates with little change in their size until concentrations closer to the binodals are reached.

The variation in micelle diameters between ABS and AcABS shown in Fig. 4B is attributed to the difference in Na^+ and H_3O^+ interactions with [P_{44414}]$^+$ due to the nature of H_3O^+. An analysis of the charge distribution at the molecular surface of H_3O^+ (Fig. S3, ESI†) shows that, in contrast to water which has a partial negative charge on the oxygen, a significant portion of the positive charge resides on the oxygen atom of H_3O^+. This entails that although H_3O^+ can donate three hydrogen bonds to neighbouring water molecules, it can no longer act as a good hydrogen-bond acceptor giving H_3O^+ an amphiphilic character. This behaviour is consistent with the reported accumulation of hydronium cations at the air–water interface, which is well correlated with the cation adsorption behaviour at hydrophobic surfaces.[33,44] Whilst the greater salting-out potential of Na^+ suggests that the latter resides in the bulk solution, the amphiphilic nature of H_3O^+ allows for greater interaction with the [P_{44414}]$^+$ micelle surface. This increased interaction between [P_{44414}]$^+$ and H_3O^+ results in a decrease of the hydrophobic effect and explains the low salting-out potential of HCl compared to the other tested salts.

Comparison of ABS *versus* AcABS – the influence of temperature

Gras *et al.*[9] demonstrated the temperature dependency of the [P_{44414}]Cl–HCl AcABS with the existence of a lower critical solution temperature (LCST). To further the comparison

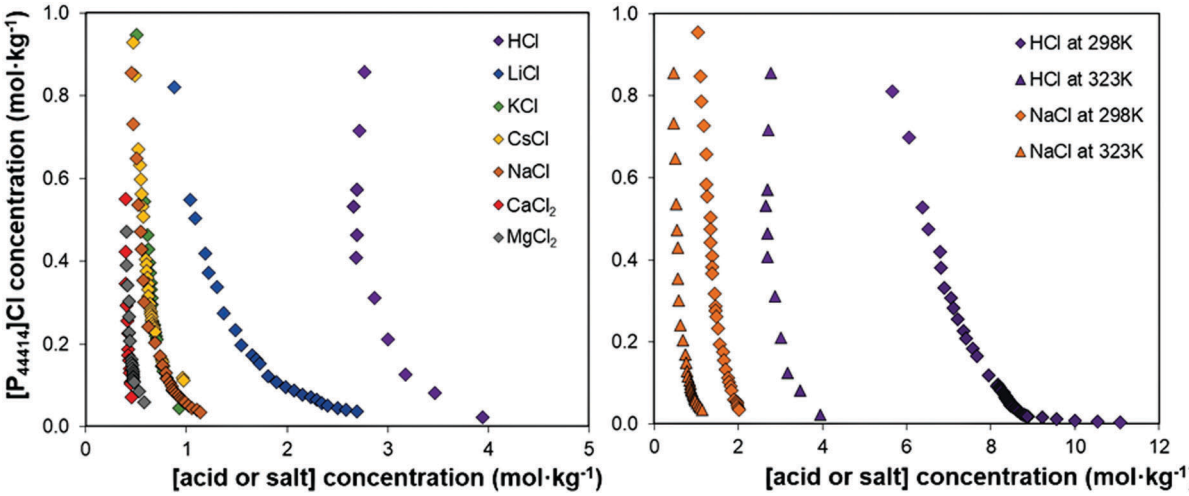

Fig. 5 Left: Binodal curves for the ABS and AcABS composed of HCl, LiCl, NaCl, KCl, CsCl, $MgCl_2$ and $CaCl_2$ with $[P_{44414}]Cl$ at 323 K. Right: Comparison of temperature effect on the binodal of NaCl and HCl at 298 K and 323 K.

between ABS and AcABS, the same systems reported in Fig. 3 were also determined at 323 K and are presented in Fig. 5. For all studied systems, a significant thermomorphic behaviour is observed with a significant increase in the biphasic region induced by the increase in temperature from 298 K to 323 K. Using the arbitrary $[P_{44414}]Cl$ concentration of 0.4 mol kg^{-1} (15 wt%) as a comparison point between the systems at 298 K to 323 K, the reduction in the salt/acid concentration required to induce phase separation is quantified and presented in Table 3. Significantly larger effects on the binodal position with temperature are observed for the weaker salting-out salts, with a decrease of 4.1 mol kg^{-1}, 2.31 mol kg^{-1} and 1.45 mol kg^{-1} observed for HCl, LiCl and $MgCl_2$ respectively compared to 0.82 mol kg^{-1} for NaCl when the system temperature is raised to 323 K. However, once these concentration differences are standardised with respect to the binodal concentration at 298 K (fourth column, Table 3), there appears to be little variation between the different ions of similar valency.

The LCST phenomenon is driven by unfavourable entropy of mixing caused by strong polar interactions and hydrogen-bond interactions (Sanchez and Stone, 2000). The similar behaviour of the salts on their respective binodal curves with temperature suggests that the LCST is primarily driven by the IL's cation–cation and cation–H_2O interactions with a secondary smaller effect from the nature of the salt. At 323 K, there is no longer any significant distinction between the binodals of NaCl, KCl and CsCl, implying a cation independent behaviour for these salts. At 323 K, the behaviour observed for $MgCl_2$ is in accordance with the Hofmeister series and becomes a stronger salting-out agent than the monovalent NaCl in contrast to the same system at 298 K. Similarly to the monovalent salts, the binodals of ABS with the divalent salts $MgCl_2$ and $CaCl_2$ overlap as well, confirming the interactions between $[P_{44414}]Cl$ and the solvent as the primary driver for the LCST type behaviour.

To establish if the observed deviation to the Hofmeister series is a consequence of the bulky polar head of $[P_{44414}]^+$ or its micellar behaviour, the binodal position for a single mixture point between $[P_{4444}]Br$ and LiCl, NaCl, KCl and $MgCl_2$ was determined. $[P_{4444}]Br$ was selected instead of $[P_{4444}]Cl$ as too few of the salts could induce ABS with the latter preventing a meaningful comparison between the systems. Substitution of one halide salt for another should not have a meaningful impact on the system behaviour beyond increasing its hydrophobicity, thereby enabling the comparison. In contrast to NaCl and KCl, LiCl and $MgCl_2$ are unable to salt-out $[P_{4444}]Br$ at 298 K. As such, the full series was determined at 323 K and the results are presented in Fig. S2 of the ESI.† Similarly to the $[P_{44414}]Cl$ system, the ability of the chloride salts to induce phase separation of $[P_{4444}]Br$ at 323 K follows the sequence $MgCl_2 > KCl \approx NaCl \gg LiCl$. This result combined with the inability of LiCl and $MgCl_2$ to induce phase separation of $[P_{4444}]Br$ at 298 K identifies the charge shielding induced by the bulky polar head of $[P_{44414}]Cl$ as the primary cause of the reported deviation from the Hofmeister series, and not the micelle formation.

The binodal curve for the $[P_{44414}]Cl$–HCl AcABS displays an unusual concave shape especially compared to the ABS systems here studied in which the binodal is linear for a large $[P_{44414}]Cl$ concentration range. To further probe the AcABS temperature dependency, the effect of the $[P_{44414}]Cl$ concentration on phase

Table 3 Effect of temperature on the salt/acid binodal concentrations (mol kg^{-1}) at 298 K ($C_{298\,K}$) and 323 K ($C_{323\,K}$) and their concentration difference ($C_{323-298}$) at a $[P_{44414}]Cl$ concentration of 0.4 mol kg^{-1} (no pH control)

Salt	$C_{298\,K}$	$C_{323\,K}$	$\Delta C_{323-298}$	$(\Delta C_{323-298})/C_{298\,K}$
HCl	6.79	2.69	4.10	0.60
LiCl	3.50	1.19	2.31	0.65
NaCl	1.38	0.56	0.82	0.60
KCl	1.59	0.63	0.96	0.60
CsCl	1.86	0.59	1.26	0.68
$MgCl_2$	1.85	0.41	1.45	0.78
$CaCl_2$	1.33	0.39	0.94	0.71

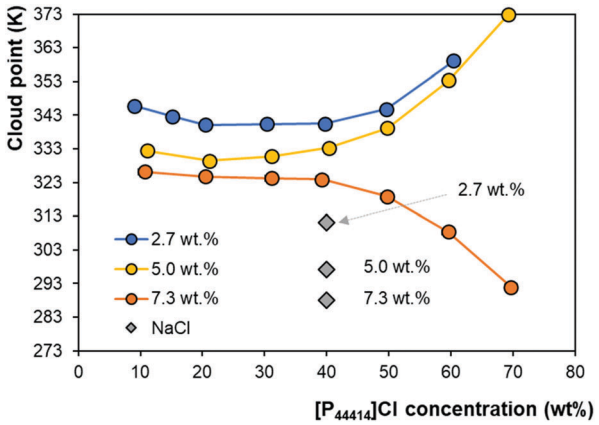

Fig. 6 Influence of $[P_{44414}]Cl$ concentration on its cloud point in the AcABS for a fixed HCl concentration and comparison with reported NaCl-based ABS.[45]

transition for a fixed HCl concentration was determined using the cloud point method and the results are presented in Fig. 6. In the binary system $[P_{44414}]Cl–H_2O$, no phase separation was observed below 398 K regardless of the IL concentration. In contrast, the addition of only 2.7 wt% HCl sharply decreases the cloud point to 342 K for a 20 wt% $[P_{44414}]Cl$ concentration. This is further decreased to 323 K when the HCl concentration is increased to 7.3 wt% HCl (2.5 M). A shift in the temperature behaviour of the $[P_{44414}]Cl–HCl$ AcABS occurs between 5 wt% HCl and 7.3 wt% HCl. In the 7.3 wt% system, there is little effect of the $[P_{44414}]Cl$ concentration on the cloud point until 50 wt% $[P_{44414}]Cl$, at which point the cloud point drops to below 273 K at 80 wt% $[P_{44414}]Cl$. The decrease of the cloud point for an identical concentration of HCl and NaCl is 303 K lower for NaCl (data point taken from ref. 45), reflecting the greater salting-out potential of the latter compared to HCl. The results in Fig. 6 show the strong effect of additives on the cloud point of aqueous $[P_{44414}]Cl$ solutions. A similar decrease in the cloud point temperature (LCST) with increased charge density of salt cations from CsCl to $MgCl_2$ was also reported for ABS with $[P_{444}C_1COOH]Cl$.[23]

Conclusions

The results reported in this work clearly evidence the outstanding potential and versatility of AcABS and hybrid AcABS–ABS systems and address the fundamental mechanisms of phase separation on these systems. The determinant structural factor for an IL's applicability in AcABS was identified as the presence of a bulky polar head in tetraalkylammonium- and phosphonium-based ILs. This finding opens exciting new applications for AcABS extractions as new ILs can now be designed with this criterion in mind. Through an experimental and computational approach, the weak salting-out ability of HCl was explored and assigned to the increased interaction of the hydronium cation with the micellar surface of the IL in aqueous solution compared to Na^+. The tunability of AcABS systems was demonstrated: all of the studied $[P_{44414}]Cl$ systems displayed a strong thermomorphic response with the presence of LCST. The ability to manipulate the formation of a biphasic system from a monophasic one and *vice versa* simply by changing the temperature avoids the kinetic limitations related to the mass transfer between two immiscible systems and extends the applicability of the reported AcABS to less acidic leachate solutions. AcABS stands out as a potential platform for the development of a more sustainable process for the separation of various strategic metals with reduced amounts of cheap and more environmentally friendly ILs compared to liquid–liquid extraction systems previously proposed based on fluorinated ions.

Conflicts of interest

There are no conflicts to declare.

Acknowledgements

This work was part of the BATRE-ARES project (ERA-MIN/0001/2015) funded by ADEME and FCT. M. Gras would like to acknowledge labex CEMAM and EIT InnoEnergy H2020 for financial support. This work was partly developed in the scope of the project CICECO – Aveiro Institute of Materials, POCI-01-0145-FEDER-007679 (FCT Ref. UID/CTM/50011/2013). Financial support from Fundação para a Ciência e a Tecnologia and Portugal 2020 to the Portuguese Mass Spectrometry Network (LISBOA-01-0145-FEDER-402-022125) is acknowledged.

Notes and references

1 J. G. Huddleston, H. D. Willauer, R. P. Swatloski, A. E. Visser and R. D. Rogers, *Chem. Commun.*, 1998, 1765.
2 C. H. C. Janssen, N. A. Macías-Ruvalcaba, M. Aguilar-Martínez and M. N. Kobrak, *Int. Rev. Phys. Chem.*, 2015, **34**, 591.
3 A. E. Visser, R. P. Swatloski, W. M. Reichert, R. Mayton, S. Sheff, A. Wierzbicki, J. H. Davis Jr. and R. D. Rogers, *Chem. Commun.*, 2001, 135.
4 A. E. Visser, R. P. Swatloski, W. M. Reichert, R. Mayton, S. Sheff, A. Wierzbicki, J. H. Davis Jr. and R. D. Rogers, *Environ. Sci. Technol.*, 2002, **36**, 2523.
5 T. P. Thuy Pham, C.-W. Cho and Y.-S. Yun, *Water Res.*, 2010, **44**, 352.
6 J. Fu, Y. I. Yang, J. Zhang, Q. Chen, X. Shen and Y. Q. Gao, *J. Phys. Chem. B*, 2016, **120**, 5194.
7 V. Mazan, M. Y. Boltoeva, E. E. Tereshatov and C. M. Folden III, *RSC Adv.*, 2016, **6**, 56260.
8 T. Vander Hoogerstraete, S. Wellens, K. Verachtert and K. Binnemans, *Green Chem.*, 2013, **15**, 919.
9 M. Gras, N. Papaiconomou, N. Schaeffer, E. Chainet, F. Tedjar, J. A. P. Coutinho and I. Billard, *Angew. Chem., Int. Ed.*, 2018, **57**, 1563.
10 A. M. Ferreira, A. F. M. Cláudio, M. Válega, F. M. J. Domingues, A. J. D. Silvestre, R. D. Rogers, J. A. P. Coutinho and M. G. Freire, *Green Chem.*, 2017, **19**, 2768.
11 C. M. S. S. Neves, S. P. M. Ventura, M. G. Freire, I. M. Marrucho and J. A. P. Coutinho, *J. Phys. Chem. B*, 2009, **113**, 5194.

12 M. J. Frisch, G. W. Trucks, H. B. Schlegel, G. E. Scuseria, M. A. Robb, *et al.*, *Gaussian 09 (revision D.01)*, Gaussian, Inc., Wallingford CT, 2009.
13 A. D. Becke, *Phys. Rev. A: At., Mol., Opt. Phys.*, 1988, **38**, 3098.
14 C. Lee, W. Yang and R. Parr, *Phys. Rev. B: Condens. Matter Mater. Phys.*, 1988, **37**, 785.
15 R. Dennington, T. A. Keith and J. M. Millam, *GaussView, Version 6*, Semichem Inc., Shawnee Mission, KS, 2016.
16 R. W. Taft and M. J. Kamlet, *J. Am. Chem. Soc.*, 1976, **98**, 2886.
17 M. A. Ab Rani, A. Brant, L. Crowhurst, A. Dolan, M. Lui, N. H. Hassan, J. P. Hallett, P. Hunt, H. Niedermeyer, J. M. Perez-Arlandis, M. Schrems, T. Welton and R. Wilding, *Phys. Chem. Chem. Phys.*, 2011, **13**, 16831.
18 K. A. Kurnia, F. Lima, A. F. M. Cláudio, J. A. P. Coutinho and M. G. Freire, *Phys. Chem. Chem. Phys.*, 2015, **17**, 18980.
19 F. A. e Silva, J. F. B. Pereira, K. A. Kurnia, S. P. M. Ventura, A. M. S. Silva, R. D. Rogers, J. A. P. Coutinho and M. G. Freire, *Chem. Commun.*, 2017, **53**, 7298.
20 S. Shahriari, C. M. S. S. Neves, M. G. Freire and J. A. P. Coutinho, *J. Phys. Chem. B*, 2012, **116**, 7252.
21 K. A. Kurnia, M. G. Freire and J. A. P. Coutinho, *J. Phys. Chem. B*, 2014, **118**, 297.
22 L. G. Sillén, A. E. Martell and J. Bjerrum, *Stability constants of metal–ion complexes*, Chemical Society, London, 1964.
23 D. Dupont, D. Depuydt and K. Binnemans, *J. Phys. Chem. B*, 2015, **119**, 6747.
24 Y. Marcus, *Chem. Rev.*, 2009, **109**, 1346.
25 N. Schwierz, D. Horinek and R. R. Netz, *Langmuir*, 2010, **26**, 7370.
26 N. Schwierz, D. Horinek and R. R. Netz, *Langmuir*, 2013, **29**, 2602.
27 N. Schwierz, D. Horinek and R. R. Netz, *Langmuir*, 2015, **31**, 215.
28 N. Schwierz, D. Horinek, U. Sivan and R. R. Netz, *Curr. Opin. Colloid Interface Sci.*, 2016, **23**, 10.
29 M. G. Freire, C. M. S. S. Neves, A. M. S. Silva, L. M. N. B. F. Santos, I. M. Marrucho, L. P. M. Rebelo, J. K. Shah, E. J. Maginn and J. A. P. Coutinho, *J. Phys. Chem. B*, 2010, **114**, 2004.
30 R. K. Blundell and P. Licence, *Phys. Chem. Chem. Phys.*, 2014, **16**, 15278.
31 X. Liu, Y. Zhao, X. Zhang, G. Zhou and S. Zhang, *J. Phys. Chem. B*, 2012, **116**, 4934.
32 M. Goergenyi, J. Dewulf, H. Van Langenhove and K. Heberger, *Chemosphere*, 2006, **65**, 802.
33 L. M. Pegram and M. T. Record Jr., *J. Phys. Chem. B*, 2007, **111**, 5411.
34 X. Wen-Hui, S. Jing-Zhe and X. Xi-Ming, *Thermochim. Acta*, 1990, **169**, 271.
35 D. L. Beauchamp and M. Khajehpour, *Biophys. Chem.*, 2012, **163-164**, 35.
36 H. Schott, A. E. Royce and S. K. Han, *J. Colloid Interface Sci.*, 1984, **98**, 196.
37 M. Kumbhakar, T. Goel, T. Mukherjee and H. Pal, *J. Phys. Chem. B*, 2005, **109**, 18528.
38 M. Kumbhakar, T. Mukherjee and H. Pal, *Chem. Phys. Lett.*, 2005, **413**, 142.
39 A. S. Thomas and A. H. Elcock, *J. Am. Chem. Soc.*, 2007, **129**, 14887.
40 L. Pauling, *The nature of the chemical bond*, Cornell University Press, Ithaca, NY, 1960.
41 G. D. Markham, J. P. Glusker and C. W. Bock, *J. Phys. Chem. B*, 2002, **106**, 5118.
42 T. Dudev and C. Lim, *J. Am. Chem. Soc.*, 2013, **135**, 17200.
43 W. L. Hinze and E. Pramauro, *Crit. Rev. Anal. Chem.*, 1993, **24**, 133.
44 P. Ball, *Chem. Rev.*, 2008, **108**, 74.
45 B. Onghena, T. Opsomer and K. Binnemans, *Chem. Commun.*, 2015, **51**, 15932.

